IEEE Photonics Journal
An IEEE Photonics Society Publication

Open Access

Monolithically Integrated 4-Channel-Selectable Light Sources Fabricated by the SAG Technology

Volume 5, Number 4, August 2013

Can Zhang
Hongliang Zhu
Song Liang
Liangshun Han
Wei Wang

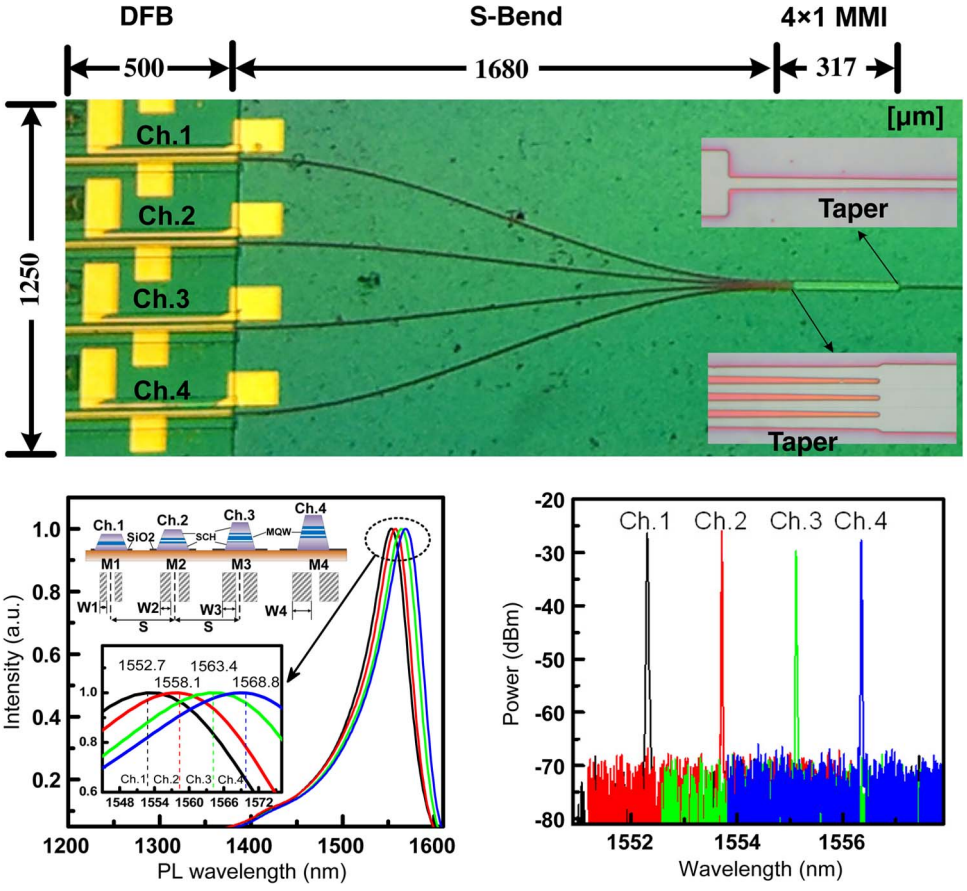

DOI: 10.1109/JPHOT.2013.2271733
1943-0655/$31.00 ©2013 IEEE

Monolithically Integrated 4-Channel-Selectable Light Sources Fabricated by the SAG Technology

Can Zhang, Hongliang Zhu, Song Liang, Liangshun Han, and Wei Wang

Key Laboratory of Semiconductor Material Sciences, Institute of Semiconductors, Chinese Academy of Sciences, Beijing 100083, China

DOI: 10.1109/JPHOT.2013.2271733
1943-0655/$31.00 ©2013 IEEE

Manuscript received May 4, 2013; revised June 9, 2013; accepted June 16, 2013. Date of publication July 4, 2013; date of current version July 10, 2013. This work was supported in part by the National 863 Project under Grant 2011AA010303; by the National Natural Science Foundation of China under Grants 61090392, 60736036, and 61021003; and by the National 973 Program under Grant 2011CB301702. Corresponding authors: H. L. Zhu and C. Zhang (e-mail: zhuhl@semi.ac.cn; zhangcan537@semi.ac.cn).

Abstract: The monolithic integration of four 1.5-μm InGaAsP/InP distributed feedback (DFB) lasers with a 4 $\times$ 1 multimode-interference (MMI) optical combiner using the selective area growth and butt-joint regrowth technologies is proposed and demonstrated. A dry-etching stop layer is grown to guarantee the etching depth of MMI. The four channels could match the ITU wavelength grid of 200-GHz well with a simple integrated thin-film heater, covering the wavelength range of 1552.3–1556.3 nm. The average output power of LD is 2.8 mW with a 150-mA current, and the threshold current is 20–22 mA at 25 °C. The four channels can operate separately or simultaneously.

Index Terms: Laser array, multiwavelength light sources, thin-film heater.

1. Introduction

InP-based large-scale photonic integrated circuits (LS-PICs) have been successfully deployed in optical transport networks [1]. Multi-wavelength light sources are now key components in dense wavelength division multiplexing optical transmission systems and are indispensable in future photonic networks [2]–[4]. There are several methods of multi-wavelength laser sources reported: multi-section distributed Bragg reflector (DBR) laser diodes [5], arrayed waveguide grating (AWG) laser diodes [6], distributed feedback (DFB) laser array [7]–[9] and integrated devices with multi-mode interference coupler and a semiconductor optical amplifier integrated [10]–[13].

The monolithic distributed feedback (DFB) laser arrays are widely used for their stable and highly reliable single-mode operation in modern wavelength division multiplexing (WDM) system. The lasing wavelength is determined by the pitch of the built-in grating along the laser cavity together with the waveguide effective refractive index. Several techniques have been proposed for the fabrication of DFB laser array according these two factors mentioned above, such as electron beam lithography [14], ridge width variation [15], ridge tilt [16], multiple holographic exposures [17], and sampled gratings [18]. However, most of these techniques referred here require high costs and rather harsh manufacture process. The single-mode-yield is the most important thing for the large-scale photonic integrated circuits (LS-PIC). So a simple fabrication technology is urgently required for high-yield DFB laser array production. Selective area growth (SAG) of multi-quantum wells

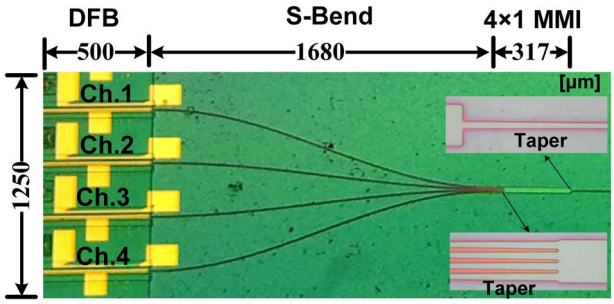

Fig. 1. Optical microscope picture of the integrated device.

(MQWs) by metal organic vapor phase epitaxy (MOVPE) is another and an attractive one [19], [20], because only a relatively simple procedure is needed. This SAG technique grows epitaxial layers in areas between dielectric masks. The thickness enhancement factors of selectively grown layers are affected by the geometry of mask patterns including mask widths and mask gap between two adjacent mask patterns. The effective refractive index of MQWs could be controlled by modulating the thickness of the waveguide layer, which could realize the controlling of lasing wavelength.

In this paper, a four channel DFB laser array integrated MMI combiner is proposed and demonstrated by SAG and butt-joint regrowth (BJR) technologies. The integrated device is fabricated by conventional holographic method with constant-pitch grating. The four channels could match well the ITU wavelength grid of 200 GHz with an integrated thin-film heater.

2. Design and Fabrication

The optical microscope photograph of the fabricated device is shown in Fig. 1. The total integrated chip size is about 2600 $\times$ 1250 μm^2. The DFB laser section is 500 μm long, which is fabricated by SAG technology. The separation between two adjacent lasers is set at 250 μm in order to decrease the electrical and thermal crosstalk. The S-bend patterns are 1680 μm long to decrease radiation loss. The sensitivity to optical feedback is important for the laser using in optical transmission system [21], [22]. Two measures are taken for the device to reduce the optical reflections. One is the design of shallow ridged waveguide for MMI to reduce the reflections from shallow-deep waveguide transitions. The other is the tapered input and output waveguides, which are used to reduce the back reflections at the input waveguides of MMI and improve the uniformity of output power [23]. The 4 $\times$ 1 MMI coupler with tapered input/output waveguides is designed to be 24 μm wide to satisfy the waveguide separation at the MMI entrances. The MMI length is calculated as 317 μm long by 3-D BeamPROP analysis software. The widths of ridge waveguide for both laser and MMI are 3 μm.

The fabrication processes are composed of three step metal organic vapor phase epitaxy (MOVPE) growths: selective area growth (SAG), butt-joint regrowth (BJR), and P-contact layer growth. The SAG technology was applied to grow selectively different MQW active structures aiming to fabricate the multi-wavelength DFB-LD array [24]. Fig. 2(a) shows the SEM picture of SAG morphology. The passive MMI region was then selectively etched down until InP buffer layer and a thin InP layer and InGaAsP waveguide core layer was regrown by the BJR technique, as shown in Fig. 2(b).

For the fabrication of laser by SAG process, the dielectric masks used for the SAG study were SiO_2 grown by plasma enhanced chemical vapor deposition (PECVD). The thickness of the film is 150 nm. The width of the mask gap is kept constant at 20 μm and the width of mask strips (W_m) ranges from 21.75 μm to 26.97 μm in 1.74 μm increment, as shown in Fig. 3. The MQWs are then grown on the patterned wafer, which consist of 6 compressively strained InGaAsP wells, 7 InGaAsP barrier layers and are sandwiched between two 80 nm InGaAsP separate confinement heterostructure (SCH) layers. Two thin p doped and n doped InGaAsP layers were grown successively on the upper SCH layer, which induce a weak gain coupling into the DFB structure

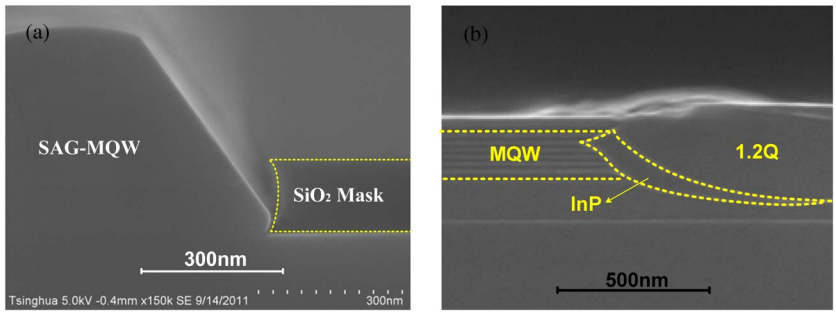

Fig. 2. (a) SEM picture of SAG morphology for LDs, (b) butt-joint regrowth for active/passive region.

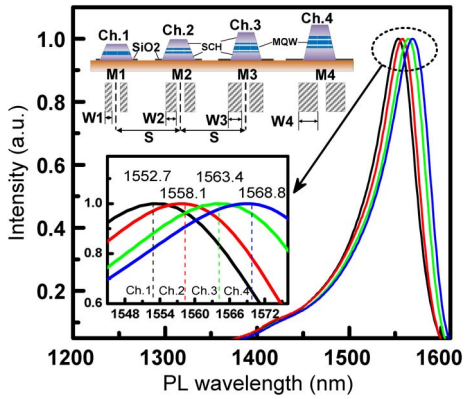

Fig. 3. Distribution of PL wavelength of four-channel laser regions.

and helps to increase the rate of single mode lasing. The temperature and the pressure during the MOVPE growth are 640 °C and 100 mbar, respectively. On unpatterned substrates, the thickness of the well and barrier are 5 nm and 10 nm, respectively. It is found that the photoluminescence (PL) emission wavelength in the SAG region exhibits a red shift correlating to the mask patterns, as shown in Fig. 3. From our previous experiments [24], it can be found that the thickness enhancement of SCH layer could be approximately deduced by the red-shift of PL wavelength, which determines the channel spacing of DFB laser. Fig. 3 shows the distribution of PL wavelength of four-channel laser region. The interval of the PL wavelength between the adjacent channels is about 5.36 nm, which induces a corresponding refractive-index variation of ridge waveguide. After the SAG process was finished, the BJR technique was conducted to grow the core-layer material of MMI. As the first step, SiO_2 stripe patterns were defined to secure the active region. Then, the passive region was selectively etched down until InP buffer layer by reaction ion etching (RIE) with the CH_4/H_2 gas mixture. After the treatment of a slight chemical cleaning for 20 s in dilute HBr solution, a 300 nm-thick MMI core layer was selectively grown. For the passive MMI structure is sensitive to the etching depth and roughness of waveguide sidewall, it is fabricated as shallow-ridge waveguide. A thin AlGaInAs layer (about 10 nm-thick) was inserted between the upper and lower InGaAsP core layer, which could realize the functionality of etching stop layer due to large selectivity to InGaAsP in RIE process and had a small impact on our design of MMI structure. Fig. 4 shows the distribution of PL wavelength for MMI core layer with InGaAsP layer-1194.62 nm and AlGaInAs layer-1330.12 nm.

After finishing the butt-joint regrowth, a grating with a uniform pitch was selectively fabricated on the laser region by holographic lithograph technology. Then, a third epitaxy growth was followed, including a p-type InP cladding layer and a p^+ InGaAs contact layer. The ridge waveguides of laser and MMI were formed simultaneously by RIE process, which could realize the depth control with

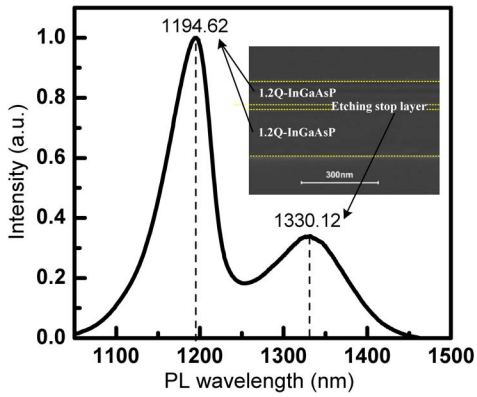

Fig. 4. PL wavelength of butt-joint MMI core layer.

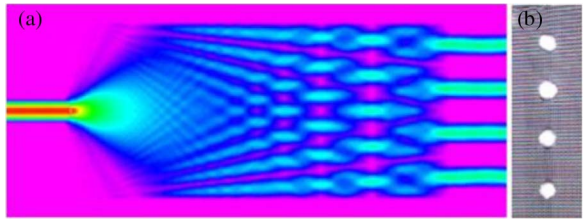

Fig. 5. (a) Simulated input characteristic of MMI, (b) experimental results of infrared spots.

proper gas sources ($CH_4/H_2/O_2$ gas mixture) by the etching stop layer. A 450 nm SiO_2 layer was deposited by PECVD to cover the entire wafer and SiO_2 openings over the ridges were formed by wet etching. Then 200 nm Ti and 400 nm Au layers were deposited successively in a single sputter run on the p-side of the device for the fabrication of p-electrode and thin-film strip heaters. With two-step photolithography process, Ti thin-film heaters and Ti-Au p-contacts of laser and heaters were formed together. AuGeNi alloy was deposited as n-contact metal after the wafer was thinned to about 200 μm. All output facets of the device structure were formed by cleaving without additional dielectric coating.

3. Characteristics of Integrated Device

Considering the level of our etching equipment, shallow ridge waveguide were designed to reduce the propagation loss of long S-bend waveguide. The input characteristics of 4 $\times$ 1 MMI coupler were calculated by 3-D analysis BeamPROP software. Fig. 5(a) and (b) show the simulated and experimented input results of the MMI coupler, respectively. Four infrared spots were obtained, each uniform and clear, indicating that the MMI was properly designed.

The fabricated device was mounted onto a Cu heat sink for systematic device characterization with constant temperature kept at 25 °C. The light output power versus injection current (L-I) curves of the integrated 4-channel-selectable light sources are shown in Fig. 6, which are tested by coupling lights into single-mode tapered lens-fibers. The light power of laser facet and MMI output port are shown in Fig. 6(a) and (b), respectively. The average slope efficiency of the MMI output port was 0.023 W/A and the threshold was 20-22 mA, while the DFB facets was 0.174 W/A and the threshold was 20-22 mA. The difference between the two devices comes from the radiation loss, the transmission loss of passive waveguide and the direct bandgap absorption in the passive region. The total losses for four channels were between 8.57 and 8.92 dB. The optical loss included butt-joint coupling, the inherent loss of 1-by-4 MMI coupler (6 dB) and the propagation loss of waveguide.

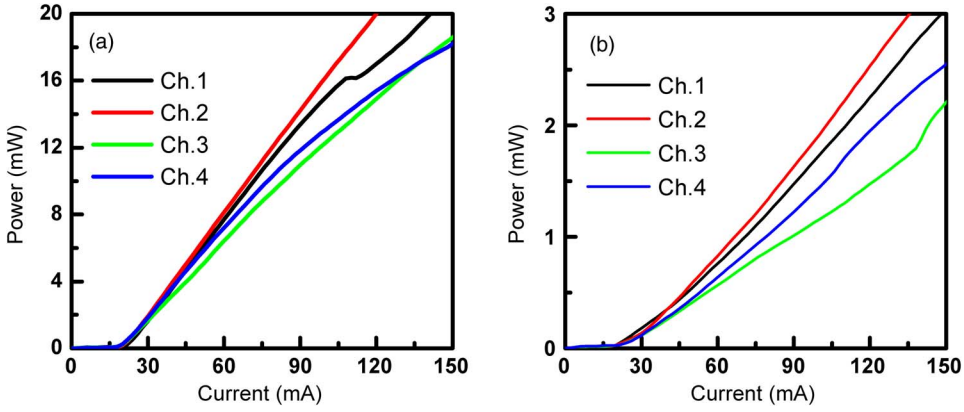

Fig. 6. Four-channel L–I characteristics of (a) DFB facets and (b) MMI output port.

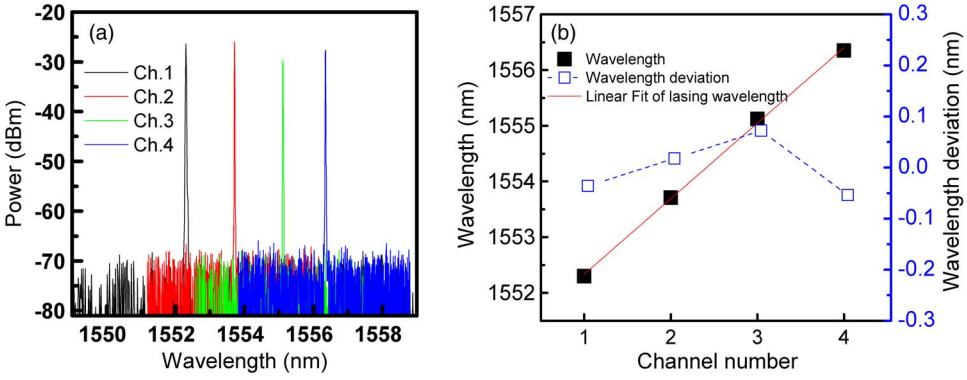

Fig. 7. (a) Superimposed output spectra of the integrated device and (b) the wavelength deviation from the fitted value of each channel.

The superimposed output spectra of the four-channel-selectable light sources fabricated by the SAG and BJR process are shown in Fig. 7(a). As can be seen, the side-mode-suppression-ratios (SMSR) of all the channels are larger than 40 dB. The emission wavelength as a function of channel number is shown in Fig. 7(b) and can be fitted well with a linear curve, which has an average channel spacing 1.356 nm. The wavelength deviation from the fitted value of each channel is shown in Fig. 7(b), which is less than 0.1 nm. Small current tuning could make fine wavelength alignment. The real and imaginary parts of the coupling coefficient of the laser element with the DFB laser, estimated by the method in ref [25], are 38 and 6 cm^{-1}, respectively, rendering a κL of 1.9. Our results show that SAG technique which is promising for reducing cost of laser array can be used for the fabrication of multi-channel light sources with very good uniformity of wavelength spacing. The channel spacing of the integrated device can thus be tuned by the geometry of mask patterns including mask width and separation to satisfy the required spacing. Each laser has also an integrated Ti thin-film heater owing a tuning range about 5.0 nm. Proper heater current is applied to each heater of the laser to match the ITU grid of 200 GHz, as shown in Fig. 8. In Dense-WDM systems, multiple DFB-LDs in the array operate simultaneously. Therefore, the design of 250 μm-increment LDs contributes to very low crosstalk between adjacent channels.

4. Conclusion

A monolithic integration of four 1.55-μm DFB lasers with a 4 $\times$ 1 MMI optical combiner using the SAG and BJR method is proposed and demonstrated. The typical threshold current is about 20 mA

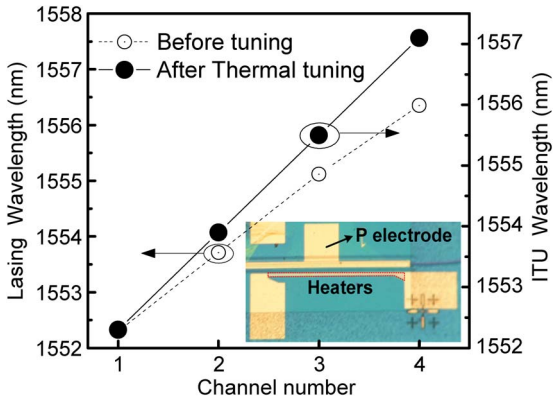

Fig. 8. Wavelength distribution before and after thermal tuning.

and the average output power for each channel is 2.8 mW with the LD current of 150 mA. The average channel spacing of the selectable light sources is about 1.356 nm with uniform spacing. The four channels can operate separately or simultaneously, which could satisfy the 200 GHz ITU grid with the integrated Ti thin-film heaters. This device is promising for wide use in compact transmitter modules for 10-Gb/s four-channel DWDM network systems.

References

[1] R. Nagarajan, M. Kato, J. Pleumeekers, P. Evans, D. Lambert, A. Chen, V. Dominic, A. Mathur, P. Chavarkar, M. Missey, A. Dentai, S. Hurtt, J. Bäck, R. Muthiah, S. Murthy, R. Salvatore, C. Joyner, J. Rossi, R. Schneider, M. Ziari, H.-S. Tsai, J. Bostak, M. Kauffman, S. Pennypacker, T. Butrie, M. Reffle, D. Mehuys, M. Mitchell, A. Nilsson, S. Grubb, F. Kish, and D. Welch, "Large-scale photonic integrated circuits for long-haul transmission and switching," *J. Opt. Netw.*, vol. 6, no. 2, pp. 102–111, Feb. 2007.

[2] S. Corzine, P. Evans, M. Fisher, J. Gheorma, M. Kato, V. Dominic, P. Samra, A. Nilsson, J. Rahn, I. Lyubomirsky, A. Dentai, P. Studenkov, M. Missey, D. Lambert, A. Spannagel, R. Muthiah, R. Salvatore, S. Murthy, E. Strzelecka, J. L. Pleumeekers, A. Chen, R. Schneider, R. Nagarajan, M. Ziari, J. Stewart, C. H. Joyner, F. Kish, and D. F. Welch, "Large-scale InP transmitter PICs for PM-DQPSK fiber transmission systems," *IEEE Photon. Technol. Lett.*, vol. 22, no. 14, pp. 1015–1017, Jul. 2010.

[3] T. Fujisawa, S. Kanazawa, K. Takahata, W. Kobayashi, T. Tadokoro, H. Ishii, and F. Kano, "1.3-μm, 4$\times$ 25-Gbit/s, EADFB laser array module with large-output-power and low-driving-voltage for energy-efficient 100GbE transmitter," *Opt. Exp.*, vol. 20, no. 1, pp. 614–620, Jan. 2012.

[4] T. Fujisawa, T. Itoh, S. Kanazawa, K. Takahata, Y. Ueda, R. Iga, H. Sanjo, T. Yamanaka, M. Kotoku, and H. Ishii, "Ultracompact, 160-Gbit/s transmitter optical subassembly based on 40-Gbit/s $\times$ 4 monolithically integrated light source," *Opt. Exp.*, vol. 21, no. 1, pp. 182–189, Jan. 2013.

[5] W. Jia, Y. Matsui, D. Mahgerefteh, I. Lyubomirsky, and C. K. Chan, "Generation and transmission of 10-Gbaud optical 3/4-RZ-DQPSK signals using a chirp-managed DBR laser," *J. Lightw. Technol.*, vol. 30, no. 21, pp. 3299–3305, Nov. 2012.

[6] Y. Suzaki, H. Yasaka, H. Mawatari, K. Yoshino, Y. Kawaguchi, S. Oku, R. Iga, and H. Okamoto, "Monolithically integrated eight-channel WDM modulator with narrow channel spacing and high throughput," *IEEE J. Sel. Topics Quantum Electron.*, vol. 11, no. 1, pp. 43–49, Jan./Feb. 2005.

[7] C. Zhang, S. Liang, L. Ma, B. J. Wang, H. L. Zhu, and W. Wang, "A modified SAG technique for the fabrication of DWDM DFB laser arrays with highly uniform wavelength spacings," *Opt. Exp.*, vol. 20, no. 28, pp. 29620–29625, Dec. 2012.

[8] S.-W. Ryu, S.-B. Kim, J.-S. Sim, and J. Kim, "Asymmetric sampled grating laser array for a multiwavelength WDM source," *IEEE Photon. Technol. Lett.*, vol. 14, no. 12, pp. 1656–1658, Dec. 2002.

[9] G. W. Yoffe, S. Y. Zou, B. Pezeshki, S. A. Rishton, and M. A. Emanuel, "High-precision high-yield laser source using DFB array," *IEEE Photon. Technol. Lett.*, vol. 16, no. 3, pp. 735–737, Mar. 2004.

[10] K. Kudo, K. Yashiki, T. Sasaki, Y. Yokoyama, K. Hamamoto, T. Morimoto, and M. Yamaguchi, "1.55-μm wavelength-selectable microarray DFB-LD's with monolithically integrated MMI combiner, SOA, and EA-modulator," *IEEE Photon. Technol. Lett.*, vol. 12, no. 3, pp. 242–244, Mar. 2000.

[11] K. Yashiki, K. Sato, T. Morimoto, S. Sudo, K. Naniwae, A. Satoshi, K. Shiba, N. Suzuki, T. Sasaki, and K. Kudo, "Wavelength-selectable light sources fabricated using advanced microarray-selective epitaxy," *IEEE Photon. Technol. Lett.*, vol. 16, no. 7, pp. 1619–1621, Jul. 2004.

[12] N. Nunoya, H. Ishii, Y. Kawaguchi, R. Iga, T. Sato, N. Fujiwara, and H. Oohashi, "Tunable distributed amplification (TDA-) DFB laser with asymmetric structure," *IEEE J. Sel. Topics Quantum Electron.*, vol. 17, no. 6, pp. 1505–1512, Nov./Dec. 2011.

[13] N. Nunoya, H. Ishii, Y. Kawaguchi, Y. Kondo, and H. Oohashi, "Wide band tuning of tunable distributed amplification distributed feedback laser array," *Electron. Lett.*, vol. 44, no. 3, pp. 205–207, Jan. 2008.
[14] K. Kudo, T. Morimoto, K. Yashiki, T. Sasaki, Y. Yokoyama, K. Hamamoto, and M. Yamguchi, "Wavelength-selectable microarray light sources of multiple ranges simultaneously fabricated on single wafer," *Electron. Lett.*, vol. 36, no. 8, pp. 745–747, Apr. 2000.
[15] G. P. Li, T. Makino, A. Sarangan, and W. Huang, "16-wavelength gain-coupled DFB laser array with fine tunability," *IEEE Photon. Technol. Lett.*, vol. 8, no. 1, pp. 22–24, Jan. 1996.
[16] A. M. Sarangan, W. P. Huang, G. P. Li, and T. Makino, "Selection of transverse oscillation modes in tilted ridge DFB lasers," *J. Lightw. Technol.*, vol. 14, no. 8, pp. 1853–1858, Aug. 1996.
[17] C. E. Zah, F. J. Favire, B. Pathak, R. Bhat, C. Caneau, P. S. D. Lin, A. S. Gozdz, N. C. Andreadakis, M. A. Koza, and T. P. Lee, "Monolithic integration of multiwavelength compressive-strained multiquantum-well distributed-feedback laser array with star coupler and optical amplifiers," *Electron. Lett.*, vol. 28, no. 25, pp. 2361–2362, Dec. 1992.
[18] H. L. Zhu, X. D. Xu, H. Wang, D. H. Kong, S. Liang, L. J. Zhao, and W. Wang, "The fabrication of eight-channel DFB laser array using sampled gratings," *IEEE Photon. Technol. Lett.*, vol. 22, no. 5, pp. 353–355, Mar. 2010.
[19] M. Aoki, T. Taniwatari, M. Suzuki, and T. Tsutsui, "Detuning adjustable multiwavelength MQW-DFB laser array grown by effective index/quantum energy control selective area MOVPE," *IEEE Photon. Technol. Lett.*, vol. 6, no. 7, pp. 789–791, Jul. 1994.
[20] Y. Katoh, T. Kunii, Y. Matsui, H. Wada, T. Kamijoh, and Y. Kawa, "DBR laser array for WDM system," *Electron. Lett.*, vol. 29, no. 25, pp. 2195–2197, Dec. 1993.
[21] F. Grillot, B. Thedrez, and G.-H. Duan, "Feedback sensitivity and coherence collapse threshold of semiconductor DFB lasers with complex structures," *IEEE J. Quantum Electron.*, vol. 40, no. 3, pp. 231–240, Mar. 2004.
[22] F. Grillot, "On the effects of an antireflection coating impairment on the sensitivity to optical feedback of AR/HR semiconductor DFB lasers," *IEEE J. Quantum Electron.*, vol. 45, no. 6, pp. 720–729, Jun. 2009.
[23] R. Hanfoug, L. M. Augustin, Y. Barbarin, J. J. G. M. van der Tol, E. A. J. M. Bente, F. Karouta, D. Rogers, S. Cole, Y. S. Oei, X. J. M. Leijtens, and M. K. Smit, "Reduced reflections from multimode interference couplers," *Electron. Lett.*, vol. 42, no. 8, pp. 465–466, Apr. 2006.
[24] C. Zhang, S. Liang, H. L. Zhu, L. Ma, B. Wang, C. Ji, and W. Wang, "Multi-channel DFB laser arrays fabricated by SAG technology," *Opt. Commun.*, vol. 300, no. 15, pp. 230–235, Jul. 2013.
[25] T. Nakura and Y. Nakano, "LAPAREX-An automatic parameter extraction program for gain and index coupled distributed feedback semiconductor lasers, and its application to observation of changing coupling coefficient with current," *IEICE Trans. Electron.*, vol. 83, no. 3, pp. 488–495, Mar. 2000.